A Multi-Sensor Positioning Method-Based Train Localization System for Low Density Line

Wei Jiang, Sirui Chen, Baigen Cai, *Senior Member, IEEE*, Jian Wang, *Member, IEEE*, Wei ShangGuan, *Member, IEEE*, and Chris Rizos

***Abstract*—The BeiDou navigation satellite system (BDS) has been widely applied in many areas, including communications, transportation, emergency rescue, public security, surveying, precise positioning, and many other industrial applications. The integration of BDS and an inertial navigation system (INS) has the ability to achieve a more consistent and accurate positioning solution. However, during long BDS outages, the performance of such an integrated system degrades because of the characteristics of the inertial measurement unit—the sensor errors accumulate rapidly with time when operated in a standalone mode. In this paper, a BDS/INS/odometer/map-matching (MM) positioning methodology for train navigation applications is proposed to solve the problem of positioning during BDS outages when trains pass through signal obstructed areas such as under bridges, inside tunnels, and through deep valleys. The seamless transition of the train operation in various scenarios can be, therefore, maintained. When the train operates in an open-sky environment, the BDS signals are available to provide accurate positioning, and the integrated BDS/INS/odometer/MM system is used to correct the INS errors using BDS measurements and to calculate the velocity using the odometer in the navigation frame so as to improve the system reliability and accuracy. In addition, the integrated system also delivers accurate positioning measurements at a high update rate. When the BDS signals are blocked, the integrated system switches to the INS/odometer/MM mode, and the integrated system corrects the INS errors by using odometer measurements. In order to evaluate the proposed system, a real experiment was conducted on the Qinghai–Tibet railway in western China. The experimental results indicate that the proposed system can provide accurate and continuous positioning results in both open-sky and BDS signal-obstructed environments.**

***Index Terms*—BeiDou navigation satellite system, INS, odometer, map-matching, seamless train localization.**

Manuscript received April 9, 2018; revised July 7, 2018; accepted September 2, 2018. Date of publication September 10, 2018; date of current version November 12, 2018. This work was supported in part by the State Key Project of Chinese Ministry of Science and Technology under Grant 2018YFB1201500, in part by the National Natural Science Foundation of China under Grant 61703034, and in part by the Beijing Natural Science Foundation under Grant 4184096. The review of this paper was coordinated by Dr. D. Cao. *(Corresponding author: Wei Jiang.)*

W. Jiang, B. Cai, J. Wang, and W. ShangGuan are with the State Key Laboratory of Rail Traffic Control and Safety and the Beijing Engineering Research Center of EMC and GNSS Technology for Rail Transportation, School of Electronic and Information Engineering, Beijing Jiaotong University, Beijing 100044, China (e-mail: weijiang@bjtu.edu.cn; bgcai@bjtu.edu.cn; wangj@bjtu.edu.cn; wshg@bjtu.edu.cn).

S. Chen is with the College of Intelligent Transportation, Zhejiang Institute of Communications, Zhejiang 311112, China, and also with the School of Electronic and Information Engineering, Beijing Jiaotong University, Beijing 100044, China (e-mail: 15120235@bjtu.edu.cn).

C. Rizos is with the School of Civil and Environmental Engineering, University of New South Wales, Sydney, N.S.W. 2052, Australia (e-mail: c.rizos@unsw.edu.au).

Color versions of one or more of the figures in this paper are available online at http://ieeexplore.ieee.org.

Digital Object Identifier 10.1109/TVT.2018.2869157

I. Introduction

THE scale of the railway network in China has expanded considerably in recent years. With the development of the "Chinese Western Development Strategy" policy and "One Belt, One Road" policy, railway construction has been accelerating in western China and neighboring countries and territories. Because of the vast territory and sparse population, the railways in China's western region are designed as Low Density Lines (LDLs). The LDLs have the characteristics of long mileage, low traffic volume, inadequate infrastructure, and simple topology, normally operated as single track [1], [2]. One example LDL is the Chinese Qinghai-Tibet railway, which is located in mountainous area of the Tibet province and Qinghai province. Qinghai-Tibet railway is the highest and the longest plateau railway in the world, with more than 300 km of depopulated zone at altitudes of more than 4000 m above sea level, see Fig. 1. Because of the harsh operation and difficult maintenance conditions, it is necessary to research the development of a rail control and operation system that has high reliability and requires little maintenance.

Train localization is significant for a railway transportation system as it provides a close link to the safety integrity requirements of the train control system. The current train control system uses an odometer, which is also known as tachometer or speedometer, and balise to provide 1-degree longitudinal (along-track) position. This method is reliable and allows easy computation of train position [3]–[5]. However, the consecutive balises should be installed limited distances apart so as to assure the confidence interval and fulfil the probability of the required Safety Integrity Level (SIL), which is 10^{-9}/h for SIL-4. The average distance is 2 km for the European Train Control System (ETCS) and the Chinese Train Control System (CTCS) [6], [7]. Hence the operation and maintenance costs associated with an odometer/balise application would be too high for many LDLs.

GNSS has attracted increasing attention for rail applications in recent years because GNSS could help reduce, or even fully replace, the trackside odometer/balise equipment. A GNSS-based Location Determination System (LDS) has been considered as a substitute for balises, designed as virtual balises, to provide the same information as physical ones [8], [9]. This concept has been included in designed modern train control

Fig. 1. Qinghai-Tibet railway.

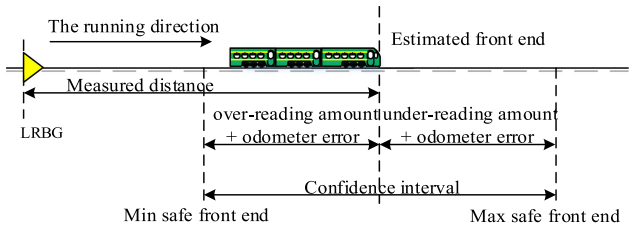

Fig. 2. Train location determination method by using odometer/balise [6].

systems, such as the Next Generation Train Control (NGTC) project, similar to the Positive Train Control (PTC) concept in North America, the European Train Control System-4 (ETCS-4) in Europe [10], and the CTCS-4 in China, to provide cost-effective solutions for local, regional and freight railway lines.

However, GNSS receivers must track more than four satellites in order to compute precise coordinates. In GNSS-difficult areas or large slope interval lines, balises and other physical equipment, are still required in order to obtain the positioning results. The integration of GNSS and an Inertial Navigation System (INS) is able to deliver a more consistent and accurate positioning capability than GNSS on its own [11], [12]. GNSS can constrain the increasing errors of INS, while INS has excellent short-term precision and aids in the mitigation of the effect of GNSS signal multipath and clock bias [13]. However, railway lines in GNSS-difficult environment are not always short. The longest tunnel in the case of the Qinghai-Tibet railway is 32 km in length. In such circumstances the performance of a GNSS/INS integrated navigation system cannot satisfy the accuracy requirement because the sensor errors of the Inertial Measurement Unit (IMU) accumulate with time when INS operates in a standalone mode [14]. In order to obtain real-time precise positioning, some form of augmented train-borne technologies is needed, such as odometers, digital track maps, Doppler velocity sensors, vision technologies and Lidar [15]. Multi-sensor technology has become an effective method to provide continuous vehicle positioning and navigation for train control systems, or even autonomous driving systems [16], [17].

Due to the one-dimensional characteristic of a railway line, map-matching (MM) can play an important role in enhancing positioning accuracy. Based on the available track geometry and positioning data, a range of mathematical methods have been utilized in MM algorithms [18]. The MM method is mainly applied to identify the rail curves [19], and computing the projecting point on the track map in order to obtain the correct train position. The railway map database contains geometric coordinates stored as discrete points, which could contribute to costly operations on regional railway lines with low traffic density [20]. The railway map database is usually compiled from different sources, such as GNSS surveys or extracted from aerial or satellite images [21].

With the BeiDou Navigation Satellite System (BDS) being able to cover the Asia-Pacific area, it has been applied in many fields in China, including communications and transportation, emergency response, public security, etc. [22], [23]. BDS can also support high accuracy navigation and positioning. Therefore in this paper a new positioning methodology based on BDS/INS/odometer/MM integration is proposed for real-time train location determination. This approach addresses the problem of train positioning during BDS outages, by providing seamless transition of train operation in different signal scenarios. When the train operates in an open-sky environment the BDS signals are available to provide accurate positioning. BDS, odometer and INS measurements are integrated to correct the INS errors with the augmentation of the MM method. The INS gyroscope and accelerometer errors are constrained by the BDS position measurements and the odometer velocity provided in the navigation frame. Furthermore, the proposed system also delivers accurate positioning at a high update rate. In the case when BDS signals are blocked the integrated system switches to the INS/odometer/MM mode. When the shortest path search algorithm is applied, the train position is projected onto the digital track map to calculate the perpendicular distance, so that the 3D coordinates in the navigation frame can be further refined.

This paper is structured as follows. The current train location determination technique is introduced in Section II. The navigation components of the proposed BDS/INS navigation system, odometer/INS navigation system and the MM method are described in Section III. The proposed system's operation in BDS open-sky and BDS-difficult scenarios is discussed in Section IV. Finally, the positioning experiment is described, and the test data analysis and evaluation results are presented.

II. Current Train Location Determination Technique

Currently, the positioning function of ETCS and CTCS is based on balise groups placed on the track as absolute reference points (LRBGs). Balise groups consist of at least two balises in most cases to ensure the information received from the balise group is applicable. In between balise groups ETCS/CTCS uses an odometer system measuring the distance traveled by the train since passing the last balise group. The odometer system calculates the distance with a guaranteed minimum performance. The maximum positioning error therefore depends on the distance from the last reference balise group. The number of balise groups used therefore depends largely on accuracy requirements. The accuracy of distances measured on-board is ± 5 m $+ 5\%$ measured distance, while the accuracy of speed is ± 2 km/h for speeds lower than 30 km/h, then increasing linearly up to ± 12 km/h at 500 km/h [6].

On an open line the distance between balise groups might be up to two kilometers or more, while in stations, where accurate stopping is required, the distance might be less than two hundred meters. Fig. 2 shows how the train position is derived from a

reference balise group and the measured distance the train has traveled since passing the balise group.

Apart from the disadvantage of the large amount of trackside equipment that needs to be installed and maintained, only longitudinal (i.e., along-track) position relative to the last balise group can be obtained. Moreover, only the trackside balise system can determine the absolute position of a train within a track layout. This is done by using the identity of the last read balise and the distance from that balise (both reported by the train), the track layout as well as the route taken by the train.

If the route is not known, when a train reports its position after startup, the calculated position might be ambiguous if one or more facing points lie within the distance from the referenced balise group to the train position. However this problem can be minimized by placing balise groups at the appropriate locations. A bigger issue exists if a train has been moved while ETCS/CTCS is not powered and therefore the balises information and distances are not obtained. In such a case the reported position might be wrong. As protection against this happening the ETCS/CTCS will only report a valid position after startup if it knows that the train has not moved. Note that most existing ETCS/CTCS trackside systems only know the track layout as shown in Fig. 2, with no reference to any absolute coordinate system such as WGS84.

III. Navigation Components and System Design

As the conventional train location determination technique is inappropriate LDLs, a BDS-based multi-sensor train localization system without wayside equipment is proposed in this paper. The components of the train navigation system are installed in the driving cab, and collect measurements from positioning sensors, including a BDS receiver, an IMU and the odometer. The information from these sensors are used to generate the positioning results with the assistance of the track map database, which is stored in the on-board map server. The location message is then transmitted to the main control unit. Fig. 3 is a schematic of a train navigation system.

In an open-sky environment, the BDS, INS, odometer measurements are fused, augmented with MM, so as to provide an accurate and reliable global navigation solution. On the other hand, only odometer and INS measurements are available to generate the navigation solution in BDS-difficult scenarios. The estimated position is calculated using odometer measurements and MM to correct the INS errors, so as to provide continuous and acceptable positioning performance.

A. BDS/INS Integrated System

The BDS/INS navigation algorithm generates position, velocity and attitude (PVA) solutions using a loosely-coupled Kalman filter (KF). PVA estimates are propagated forward in time based on IMU measurements, and errors are tracked and compensated for by utilizing an error-state KF [24].

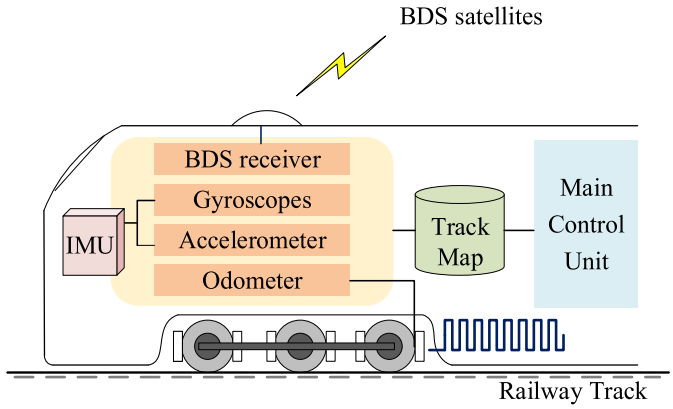

Fig. 3. Structure of the on-board train navigation system.

1) INS Update: Attitude information is maintained in the form of a transformation matrix C_b^n, relating the train body frame to the navigation frame – in this paper it is the north-east-down frame. The subscripts "b", "n", "e", "i" denote the body frame, navigation frame, earth fixed frame and inertial frame, respectively. The body coordinate frame uses the Euler rotation angles of (ϕ, θ, φ), which correspond to roll, pitch, and yaw. The initialization attitude matrix calculated by the three gyroscope measurements is given in (1), as shown at the bottom of the page.

The attitude matrix update is implemented using the quaternion approach:

$$\dot{q} = \frac{1}{2}\left[\omega_{nbq}^{b}\right] q \tag{2}$$

where q and $\dot{q}$ refer to the attitude quaternion and its rate, and ω_{nb}^{b} is the skew-symmetric matrix of the angular-rate.

Accelerometer measurements can be converted from the body frame to the navigation frame, and then used to update the position and velocity:

$$\dot{p}_n = v_n - \omega_{en}^{n} \times p_n \tag{3}$$

$$\dot{v}_n = f_n + g_n - (\omega_{en}^{n} + 2\omega_{ie}^{n}) \times v_n \tag{4}$$

where p_n and $\dot{p}_n$ are the position and position-rate vectors; v_n and $\dot{v}_n$ are the velocity and velocity-rate vectors; f_n are the accelerometer measurements; g_n is gravity; ω_{en}^{n} is the angular rate vector of the navigation frame with respect to the earth fixed frame, resolved in the navigation frame; and ω_{ie}^{n} is the angular rate vector of the earth fixed frame with respect to the inertial frame, resolved in the navigation frame.

2) Conventional BDS/INS Integrated System: The KF is used to integrate the outputs of the BDS and INS sensors. The system state of the BDS/INS integration is composed of fifteen

$$C_n^b = \begin{bmatrix} \cos\varphi\ \cos\theta & \sin\varphi\cos\theta & -\sin\theta \\ -\sin\varphi\cos\phi + \cos\varphi\ \sin\theta\ \sin\phi & \cos\varphi\cos\phi + \sin\varphi\sin\theta\sin\phi & \cos\theta\sin\phi \\ \sin\varphi\sin\phi + \cos\varphi\sin\theta\ \cos\phi & -\cos\varphi\sin\phi + \sin\varphi\sin\theta\cos\phi & \cos\theta\cos\phi \end{bmatrix} \tag{1}$$

states: attitude error (roll, pitch and yaw), position error (latitude, longitude and height), velocity error, gyroscope biases and accelerometer biases. The estimated state vector can be expressed as the motion component $X_{\psi pv}$ and the inertial sensor errors X_{ga}:

$$X = \begin{bmatrix} X_{\psi pv} & X_{ga} \end{bmatrix} = [\delta\psi \delta p_n \delta v_n \delta b_g \delta b_a] \tag{5}$$

where $\delta\psi$, δp_n, δv_n, δb_g, and δb_a are the attitude error, position error, velocity error, gyroscope biases and accelerometer biases, respectively.

The KF consists of the time-update step and the measurement-update step. The dynamic model and measurement model are:

$$X(k) = F(k-1)X(k-1) + w(k-1) \tag{6}$$

$$Z(k) = H(k)X(k) + \upsilon(k) \tag{7}$$

where $F(k-1)$ is the state transition matrix; $Z(k)$ is the system measurement matrix; $H(k)$ is the measurement matrix; $w(k-1)$ and $\upsilon(k)$ are the process noise and measurement noise, respectively, assumed to be zero-mean Gaussian noises; and the covariance matrix are $Q(k)$ and $R(k)$, respectively.

The KF time-update step propagates the system state X and the corresponding state covariance matrix P:

$$\hat{X}(k|k-1) = F(k-1)\hat{X}(k-1) \tag{8}$$

$$P(k|k-1) = F(k-1)P(k-1)F^T(k-1) + Q(k-1) \tag{9}$$

The INS navigation solution calculated during the time-update step is corrected in the measurement-update step using the longitude, latitude, altitude whenever the BDS measurements are available. The Kalman measurement-update step consists of the following operations:

$$K(k) = P(k|k-1)H^T(k)\left[H(k)P(k|k-1)H^T(k) + R(k)\right]^{-1} \tag{10}$$

$$\hat{X}(k) = \hat{X}(k|k-1) + K(k)\left[Z(k) - H(k)\hat{X}(k|k-1)\right]^{-1} \tag{11}$$

$$P(k) = [I_{15} - K(k)H(k|k-1)]\,P(k|k-1) \tag{12}$$

The measurement matrix H is calculated as:

$$H = \begin{bmatrix} 0_{3\times3} & I_{3\times3} & 0_{3\times3} & 0_{3\times6} \end{bmatrix} \tag{13}$$

The system measurement Z is calculated by comparing the position derived by BDS and the predicted position from the INS:

$$Z = [p_{BDS} - p_{INS}] \tag{14}$$

where p_{INS} is the INS position solution, and p_{BDS} is the BDS position solution.

As the BDS position solutions are from the Single Point Positioning (SPP) mode with pseudorange measurements, the positioning accuracy is typically of the order of 10 meters or better [25]. The measurement noise covariance matrix of the integrated system is dependent on the general accuracy of the system measurements. Thus the covariance of the measurement noise R_{BDS} is described by the covariance of position:

$$R_{BDS} = \text{diag}\begin{pmatrix} 3^2 & 3^2 & 3^2 \end{pmatrix} \tag{15}$$

where the unit of position covariance is m^2.

B. Odometer/INS Integration Algorithm

The use of an odometer is particularly recommended for a LDL train localization system [26], especially in areas with BDS coverage failure risk.

The odometer is used to measure the train wheel speed, from which is obtained the distance, and works together with the INS as a dead-reckoning system to determine position. The odometer can provide an estimate of absolute velocity:

$$v_{odo} = \frac{N_{odo}}{Q_{odo}} \cdot \pi \cdot d \tag{16}$$

where N_{odo} is the number of pulses per second counted by the odometer, Q_{odo} is the number of pulses when the wheel rotates a full turn, and d is the wheel diameter.

Combined with attitude matrix, the velocity in the navigation frame calculated by the odometer output is:

$$v_n = C_b^n \times \begin{bmatrix} v_{odo} & 0 & 0 \end{bmatrix}^T \tag{17}$$

The odometer/INS navigation algorithm is set up in a similar manner to the BDS/INS navigation algorithm. The system state has 15 components: attitude error (roll, pitch and yaw), position error (latitude, longitude and height), velocity error, gyroscope biases and accelerometer biases. Hence the state vector is defined as:

$$X = [\delta\psi \quad \delta p_n \quad \delta v_n \quad \delta b_g \quad \delta b_a] \tag{18}$$

Measurement Z is calculated by comparing the position obtained from the odometer, which is derived from the time integration of the odometer velocityv_n, and the predicted position derived from the INS. The odometer position is computed by multiplying the velocity in the navigation frame with the cycle time of the odometer. The measurement is:

$$Z = [p_{ODO} - p_{INS}] \tag{19}$$

where p_{INS} is the INS position solution and p_{ODO} is the position calculated using the odometer-derived velocity and the last train position information.

The measurement noise covariance of the odometer/INS integrated system is dependent on the general accuracy of the computed odometer position solution:

$$R_{ODO} = \text{diag}\begin{pmatrix} 2^2 & 2^2 & 2^2 \end{pmatrix} \tag{20}$$

where the unit of the measurement noise variance is m^2.

C. Map-Matching Algorithm

As most of railway lines in the Qinghai-Tibet Railway are designed as single track, precise train positioning using low-cost sensors and with the aid of digital maps is more suitable

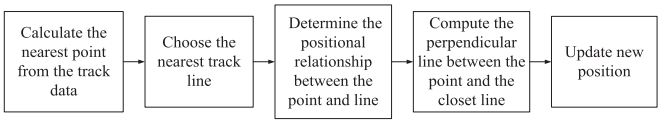

Fig. 4. The flowchart of the MM algorithm implementation.

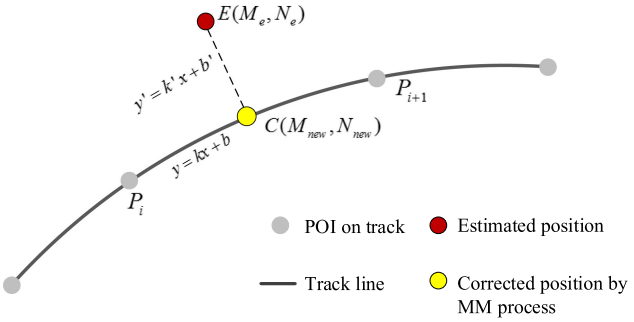

Fig. 5. The MM procedure applied to a railway track.

than conventional train positioning systems which require large amount of equipment installed along the track.

A precise track map database which carries line information is crucial for the MM method of positioning. The digital track map is defined by a series precisely measured track points. The distance between any consecutive two is of the order of several meters. The track points are then further processed through smoothing, interpolation and reduction, to generate the final rail track map.

In this paper, the shortest path search algorithm is proposed and used for single track railways. From the estimated position a vertical line is drawn down to the track railway, and the intersection point is the new estimated position.

The position of the train lies between two consecutive track points. Based on the curvature radius of the rail tracks, the trajectory between any two consecutive track points within the 1.5m interval can be assumed to be a straight line [27]. Therefore, it is comparatively easy to obtain the train position by a linear mathematical model if the positions of the two track points are known.

The proposed shortest path search based map-matching algorithm can be represented by the flowchart in Fig. 4. The nearest point-of-interest (POI) from the stored track data should be calculated first, then the nearest straight line part is chosen according to the positional relationship between the point and line. The projection is used to calculate the perpendicular distance between the point and the line, and the new position can be then be obtained.

Fig. 5 shows an example of the processing strategy. Note that the dark grey line is the railway, the light grey point is a feature point on the track, the red point is the estimated position, the black dash line is the perpendicular line which intersects the red point and the track, and the yellow point is the estimated position obtained by the MM process.

The steps are as follows:

Step 1: Estimate the position point $E(M_e, N_e)$, search the track map and calculate the nearest point from the track POI database.

Step 2: Based on the nearest point, search and determine the previous and next track points$P_i(M_i, N_i)$, $P_{i+1}(M_{i+1}, N_{i+1})$ from the track POI database. If $M_i = M_{i+1}$, go to Step 3; if$N_i = N_{i+1}$, go to Step 4; otherwise jump to Step 5.

Step 3: When $M_i = M_{i+1}$, the coordinates of the corrected position point from the MM process is:

$$M_{new} = M_i \tag{21}$$

$$N_{new} = N_e \tag{22}$$

Then go to Step 7.

Step 4: When $N_i = N_{i+1}$, the coordinates of the corrected position point from the MM process is:

$$M_{new} = M_e \tag{23}$$

$$N_{new} = N_i \tag{24}$$

Then go to Step 7.

Step 5: The straight-line equation between the two selected points of track data is:

$$y = kx + b \tag{25}$$

$$k = \frac{N_{i+1} - N_i}{M_{i+1} - M_i} \tag{26}$$

$$b = N_i M_{i+1} - N_{i+1} M_i \tag{27}$$

Step 6: Calculate the perpendicular line which intersects the point and line:

$$y' = k'x + b' \tag{28}$$

$$k' = \frac{1}{k} \tag{29}$$

$$b' = N - (k' \times M) \tag{30}$$

Step 7: Estimate the matching position point by perpendicular projection:

$$M_{new} = \frac{b' - b}{k - k'} \tag{31}$$

$$N_{new} = k \times M_{new} + b \tag{32}$$

Step 8: If a new point is received, go to Step 1.

Note there should be a perpendicular distance threshold when applying the MM approach. The position of train is on the rail track, thus choosing a suitable threshold is the key point. Firstly, the perpendicular distance from estimated position to the railway track should be calculated, then the MM processing is implemented when the perpendicular distance is less than the corresponding threshold. The appropriate threshold is determined according to the accuracy of BDS, to guarantee the effectiveness and accuracy of train positioning.

The proposed MM method can be applied to determine a train's mileage location in single track section using a simple method. However in a station scenario, the specific track where the train is parked should be determined. The track on the station can be divided as the throat part and the parallel track part, as shown in Fig. 6.

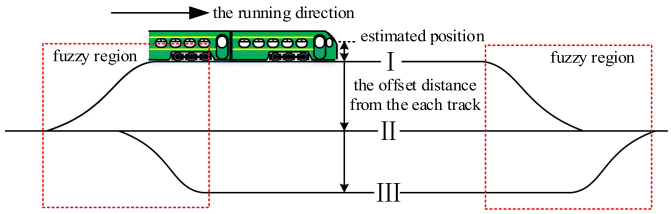

Fig. 6. Example of the fuzzy region in the station.

When the train is in the throat part of the station and the information of the track number is unknown, the fuzzy region is defined. Track fuzzy region is constructed as a safe section, where the train location can be determined by the MM method without the requirement of knowing the track number.

However when the train is in the parallel track part of the station, the track number information should be obtained. If the track number is known, the MM method is applied to calculate the projection point of the train in the corresponding track so as to correct the train location. On the other hand, if the information on the track number is not known, the offset distance between train position and each track should be calculated to determine the track number and the location of the train.

IV. System Operation in BDS-Available and BDS-Difficult Scenarios

The navigation system based on BDS, odometer and INS is expected to have good performance for both BDS-available and BDS-difficult environments. In an open-sky environment, the BDS, odometer and INS measurements are all available for positioning, and thus all measurements can be fused so as to provide an accurate and reliable global navigation solution. The global train location could then be further integrated with the digital track map to obtain a corrected on-track position. On the other hand, in BDS-difficult scenarios only odometer, INS and track map are available to generate the navigation solution. In such cases the track map can be used to assist the odometer to generate an error-corrected velocity and position, and then fused with INS measurements to obtain the system's optimal navigation solution. The train localization scheme for BDS-available and BDS-difficult environments are depicted in Fig. 7.

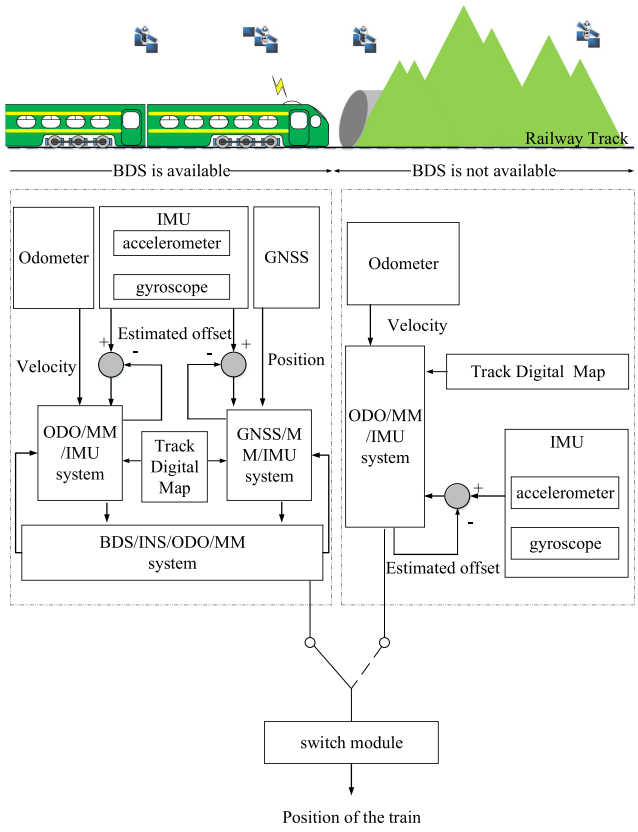

Fig. 7. Train localization schemes.

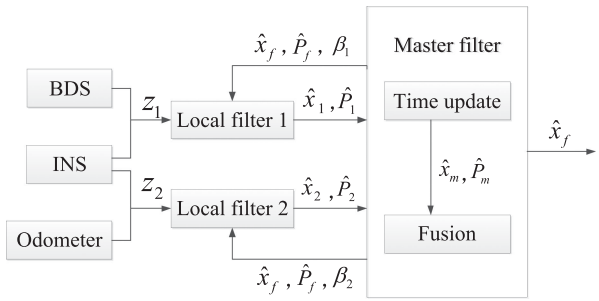

Fig. 8. System configuration of FKF which contains one master filter and two local filters (BDS/INS local filter and odometer/INS local filter).

A. BDS/Odometer/INS/MM Integrated System Operates in BDS-Available Scenario

When the train operates in an open-sky environment, BDS measurements are available. The BDS, INS and odometer measurements are fused to generate a multi-sensor navigation solution. In such cases the integrated system can generate a complete navigation solution, including position, velocity, acceleration, and attitude at high data rates.

The core component of the multi-sensor navigation system is the data fusion algorithm. The conventional data fusion algorithm used in multi-sensor navigation systems is the Centralized Kalman filter (CKF), which processes the measurements from all local sensors in one master filter, in order to generate a global optimal estimation. However a CKF has a large computational burden due to the high-dimension state computation and the large data memory requirement. The CKF also has limited reliability because of its "centralizing character" [28]–[30].

To satisfy the requirements of high reliability and low computation burden, the Federated Kalman filter (FKF) approach is often adopted as the data fusion algorithm [31], [32]. The FKF has a decentralized configuration, where the local measurements are estimated in local filters, and then the local estimates are input to a fusion space to yield the global estimation via the application of certain information fusion criteria. The system configuration of the FKF is shown in Fig. 8. It is typically a two-stage data processing algorithm, composed of one master filter and a set of local filters. Here the two local filters are the BDS/INS local filter and the odometer/INS local filter. The local filters obtain the measurements from the sensors and generate the estimates in local filters, and then the local estimates are

input into the master filter to yield a global solution. As the local filters are parallel to each other, it is easy to apply fault detection and isolation procedures. Furthermore, the FKF algorithm has a low computation load.

If the local filter and the master filter are statistically independent, they can be combined to yield the global estimates using the following information equations, where the inverse covariance is the "information matrix":

$$P_f^{-1} = P_1^{-1} + P_2^{-1} + P_m^{-1} \tag{33}$$

$$P_f^{-1}\hat{x}_f = P_1^{-1}\hat{x} + P_2^{-1}\hat{x} + P_m^{-1}\hat{x}_m \tag{34}$$

where the subscripts "1", "2", "m" and "f" denote the BDS/INS local filter, odometer/INS local filter, master filter and full filter, respectively.

In a typical FKF, the local filters and the master filter share the same system model. Thus the master filter and local filters' estimates are correlated because they use a common dynamic system. To eliminate the correlation, the covariance of the state error and process noise are set to their upper bounds:

$$\begin{cases} \hat{x}_i(k) = \hat{x}_f(k) \\ F_i(k) = F(k) \end{cases} \quad i = 1, 2, m \tag{35}$$

$$\begin{cases} \hat{P}_i^{-1}(k) = \hat{P}_f^{-1}\beta_i \\ Q_i^{-1}(k) = Q_f^{-1}\beta_i \end{cases} \quad i = 1, 2, m \tag{36}$$

where $\beta_i (\geq 0)$ is the information-sharing factors that satisfy the condition:

$$\beta_1 + \beta_2 + \beta_m = 1 \tag{37}$$

The time-updating is executed for both local filters and master filter:

$$\hat{P}_i(k|k-1) = F_i(k)\hat{P}_i(k-1)F_i^T(k) + Q_i(k); i = 1, 2, m \tag{38}$$

$$\hat{x}_i(k|k-1) = F_i(k)\hat{x}_i(k-1); i = 1, 2, m \tag{39}$$

As far as the measurement propagation is concerned, the local filters and the master filter are different:

$$K_i(k) = \hat{P}_i(k|k-1)H_i^T(k) \left[H_i(k)\hat{P}_i(k|k-1)H_i^T(k) + R_i(k)\right]^{-1}; i = 1, 2 \tag{40}$$

$$\hat{P}_i(k) = [I - K_i(k)H_i(k)]\hat{P}_i(k|k-1); i = 1, 2 \tag{41}$$

$$\hat{x}_i(k) = \hat{x}_i(k|k-1) + K_i(k)[z_i(k) - H_i(k)\hat{x}_i(k|k-1)]; i = 1, 2 \tag{42}$$

$$\hat{P}_m(k) = \hat{P}_m(k|k-1) \tag{43}$$

$$\hat{x}_m(k) = \hat{x}_m(k|k-1) \tag{44}$$

The fusion algorithm, equation (33) and (34), can be applied to combine the above local and master results:

$$\hat{P}_f^{-1}(k) = \hat{P}_m^{-1}(k) + \hat{P}_1^{-1}(k) + \hat{P}_2^{-1}(k) \tag{45}$$

$$\hat{x}(k) = \hat{P}_f(k)\left[\hat{P}_m^{-1}(k)\hat{x}_m(k) + \hat{P}_1^{-1}(k)\hat{x}_i(k) + \hat{P}_2^{-1}(k)\hat{x}_i(k)\right] \tag{46}$$

Then the global estimates are obtained.

The system model for the BDS/odometer/INS multi-sensor navigation system is the same as for the BDS/INS and odometer/INS integration systems:

$$\begin{bmatrix} \dot{x}_{\psi pv} \\ \dot{x}_{ga} \end{bmatrix} = \begin{bmatrix} F_{11} & F_{12} \\ 0_{6\times 9} & 0_{6\times 6} \end{bmatrix} \begin{bmatrix} x_{\psi pv} \\ x_{ga} \end{bmatrix} + \begin{bmatrix} 0_{9\times 1} \\ w_{ga} \end{bmatrix} \tag{47}$$

The linearized measurement equations of the BDS/INS and odometer/INS local filters are given by:

$$[\delta p_{BDS}^n - \delta p_{INS}^n] = \left[0_{3\times 3}\ I_{3\times 3}\ 0_{3\times 3}\ 0_{3\times 6}\right] x(t) + \upsilon_{BDS}(t) \tag{48}$$

$$[\delta p_{\mathrm{ODO}}^n - \delta p_{INS}^n] = \left[0_{3\times 3}\ I_{3\times 3}\ 0_{3\times 3}\ 0_{3\times 6}\right] x(t) + \upsilon_{ODO}(t) \tag{49}$$

The measurement noise covariance of the local filters are dependent on the general accuracy of the local BDS and odometer position results, which are assumed to be as in equations (15) and (20).

After the multi-sensor navigation solution is obtained, the calculated train position solution should be further combined with the digital track map data using the MM approach to generate the corrected positions.

B. System Operates in BDS-Difficult Area

When the train is operating in signal obstructed areas such as bridges, tunnels or deep valleys, the quality of the BDS signal decreases or becomes unavailable. The train positioning system monitors BDS availability and makes the decision to switch to the odometer/INS mode, and correct the INS errors by using odometer measurements. The number of visible satellites and the horizontal dilution of precision (HDOP) have a corresponding relation to the BDS-derived positioning accuracy. The greater the number of visible satellites and the smaller the value of HDOP, the better the positioning performance. Therefore the available satellite number and the HDOP are combined to determine the integration mode of the proposed multi-sensor navigation system.

The system model for the odometer/INS navigation mode can be written as in the BDS/odometer/INS multi-sensor navigation system:

$$\begin{bmatrix} \dot{x}_{\psi pv} \\ \dot{x}_{ga} \end{bmatrix} = \begin{bmatrix} F_{11} & F_{12} \\ 0_{6\times 9} & 0_{6\times 6} \end{bmatrix} \begin{bmatrix} x_{\psi pv} \\ x_{ga} \end{bmatrix} + \begin{bmatrix} 0_{9\times 1} \\ w_{ga} \end{bmatrix} \tag{50}$$

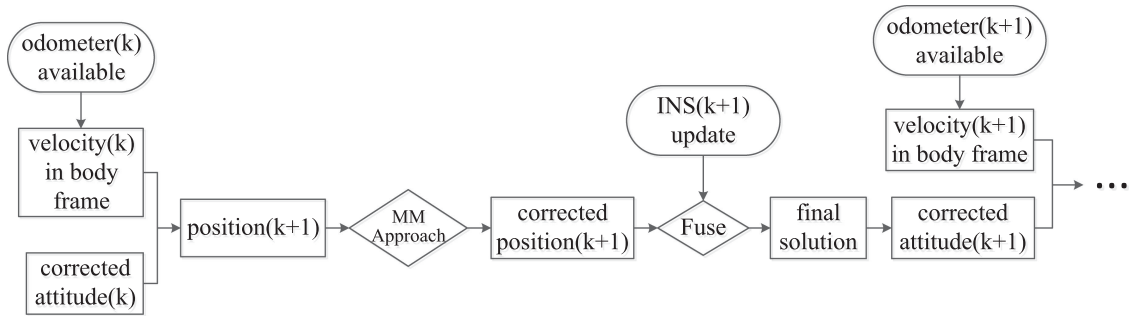

Fig. 9. System configuration when operate in BDS-difficult scenarios.

The measurement equations of the odometer/INS can be given by:

$$[\delta p^n_{\mathrm{ODO}} - \delta p^n_{INS}] = \begin{bmatrix} 0_{3\times3} & I_{3\times3} & 0_{3\times3} & 0_{3\times6} \end{bmatrix} x(t) + \upsilon_{ODO}(t) \quad (51)$$

The measurement noise covariance of the local filters are dependent on the general accuracy of the local odometer position results, which are assumed to be as in equation (20).

As the velocity measured from the odometer is in the body frame, the attitude matrix is applied to convert the velocity to the navigation frame (see equation (17)), and further obtain the odometer position. The accuracy of the attitude will influence the accuracy of odometer outputs as the error of the attitude matrix would impact on the odometer velocity and position outputs. However, the odometer update rate is typically 1 Hz or lower, which is lower than the IMU output. The inertial sensor used in this research is a low-cost micro-electromechanical system (MEMS) with sensor bias much larger than for a high accuracy INS. The odometer position output for the next epoch is calculated as soon as the odometer/INS fusion is done each time, using the corrected attitude matrix to mitigate the effect of the INS attitude error accumulation. Then when the next odometer velocity is available the calculated odometer position outputs could be fused with the INS update information.

However, even when the corrected attitude matrix is applied instead of the INS attitude update solution, the accumulated error in the attitude matrix cannot be fully eliminated. That means the corrected attitude matrix used to calculate the odometer position still has some residual bias. Therefore, in the BDS-difficult scenario described in this research, the MM approach is first applied to the calculated odometer position when each time an odometer measurement is available, which differs from the BDS-available scenarios. The corrected train location can then be generated. Then the corrected train location fuses with the INS update information to obtain an accurate final system navigation solution. The system architecture for BDS-difficult environments is depicted in Fig. 9.

V. Experiment and Result Analysis

A. Experimental Description

To evaluate the performance of the proposed navigation system a field test was conducted on the Qinghai-Tibet railway in April 2016. The experiment lasted for 20 minutes and the train travelled at approximately 70 km/h. The test trajectory is shown in Fig. 10 where it runs in mountainous areas with frequent BDS signal blockages. The test trajectory is between two adjacent stations, which are approximately 23.5 km apart.

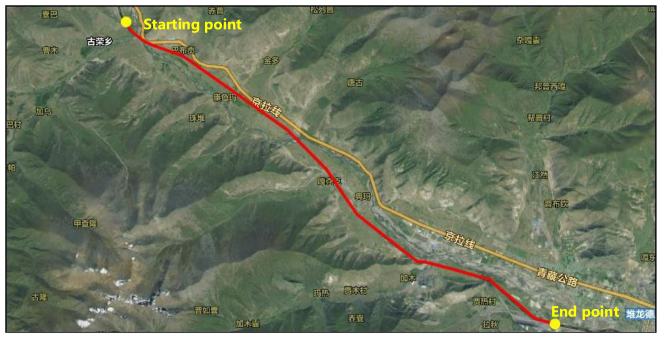

Fig. 10. The trajectory of the test conducted on the Qinghai-Tibet railway line.

Fig. 11. The test train (left) and the on-board equipment (right).

The devices that were used are: one Unicore UB370 BDS receiver, one ADIS 16488 IMU, and one odometer receiving pulse inputs from the train wheel. The BDS positioning data and IMU raw data were set at 5 Hz and 123 Hz respectively, and the odometer output rate was 1 Hz. The track map data was previously generated and stored in the map server.

The on-board equipment was installed in the driving cab, to obtain the INS measurements, odometer pulse outputs, and the BDS positioning results. The final train positioning report was transmitted to the main control unit. The left photo in Fig. 11 is the test train and the on-board equipment is shown in the right photo.

B. Position Method Evaluation

1) Evaluation of the Conventional Odometer/Balise Integrated System: Fig. 12 shows the train velocity calculated by

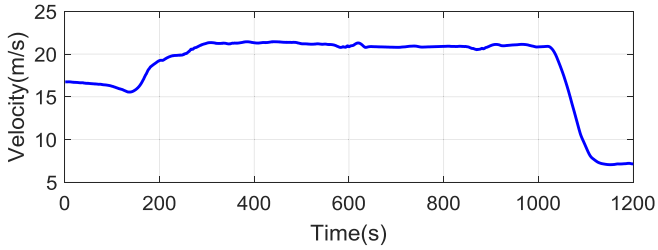

Fig. 12. The velocity of the test train during the testing period.

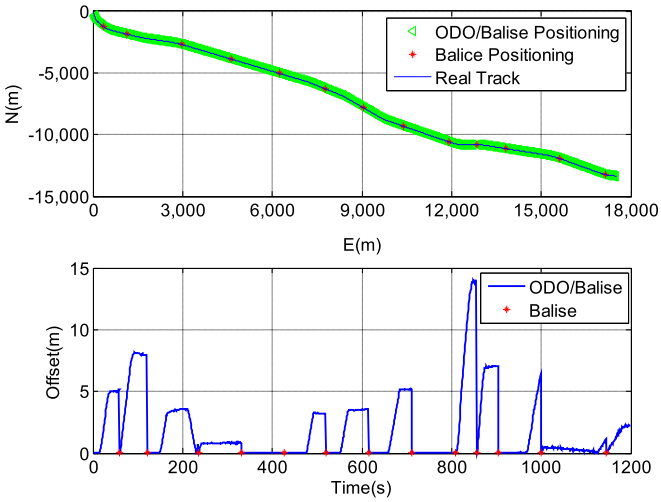

Fig. 13. Odometer/balise positioning evaluation.

the odometer. It can be seen the velocity reduced during the latter part of the test as the train runs close to the station.

Fig. 13 shows odometer/balise positioning evaluation. The top plot shows the trajectory computed by the odometer/balise integrated system. The blue solid line indicates the real track, the red line with the symbol "$*$" denotes the balise location, while the green line with the symbol "$\triangle$" is the odometer/balise integrated positioning solution, with 1 Hz output rate. The balises' locations are obtained by laboratory data simulation, which set as 2 km apart from each other for most of the test line, and 1 km in the two curve sections. According to this plot, the odometer/balise integrated system method could meet the train positioning requirements.

The bottom plot of Fig. 13 shows the offset between the odometer/balise positioning results and the real track. It can be seen during each two consecutive balises, the offset is not obvious at first, but increases rapidly with the odometer dead-reckoning, until the train passes the next balise when an absolute position correction is made.

2) Evaluation of the BDS-Based Train Positioning Method: Fig. 14 shows the positioning results obtained from the BDS SPP solutions. Plot (a) shows the trajectory computed by the BDS navigation system. It can be seen that there are three BDS-difficult areas during the testing period. Plots (b), (c) and (d) show the results during the three BDS-difficult portions of the test. The blue solid line indicates the real track data from the map database, while the red line marked with the symbol "$*$" are the BDS positioning results. The length of the three

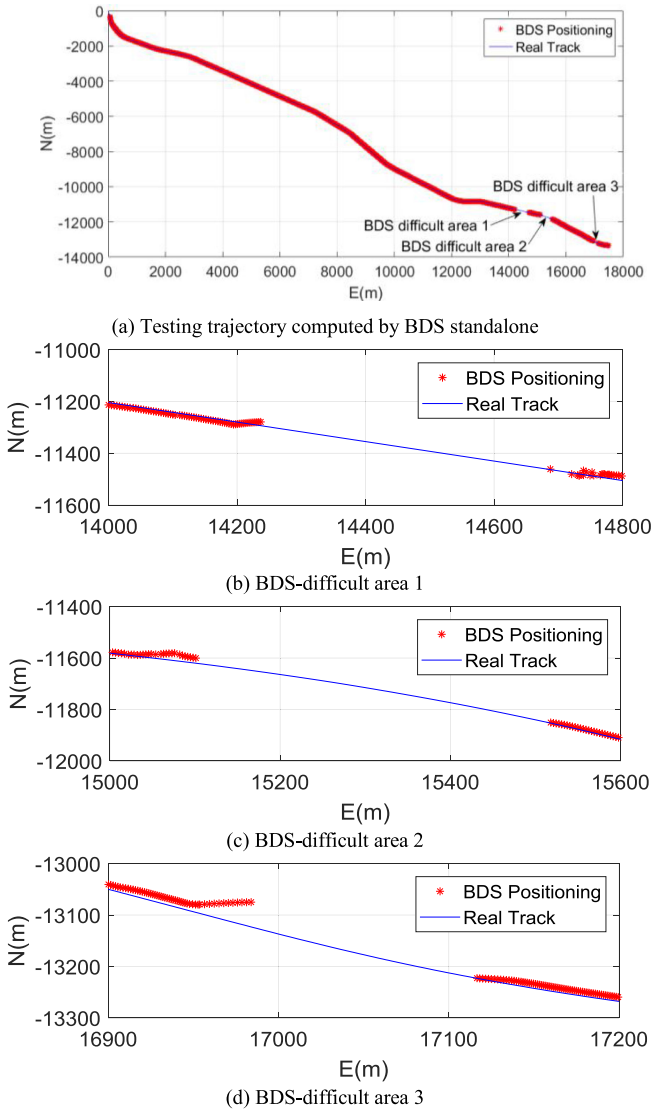

(a) Testing trajectory computed by BDS standalone

(b) BDS-difficult area 1

(c) BDS-difficult area 2

(d) BDS-difficult area 3

Fig. 14. The positioning result computed by BDS. (a) Testing trajectory computed by BDS standalone. (b) BDS-difficult area 1. (c) BDS-difficult area 2. (d) BDS-difficult area 3.

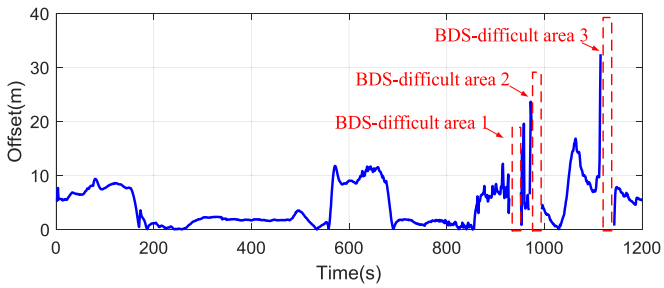

Fig. 15. The offset between BDS positioning result and the real track.

BDS-obstructed areas are about 481 m, 486, and 218 m respectively, while the time of BDS signal lock-loss period is 21.6 s, 20.2 s, and 20.4 s respectively.

Fig. 15 shows the offset between the BDS positioning results and the real track. It can be seen that the offset is large, which can be explained as the train is in mountainous areas and the

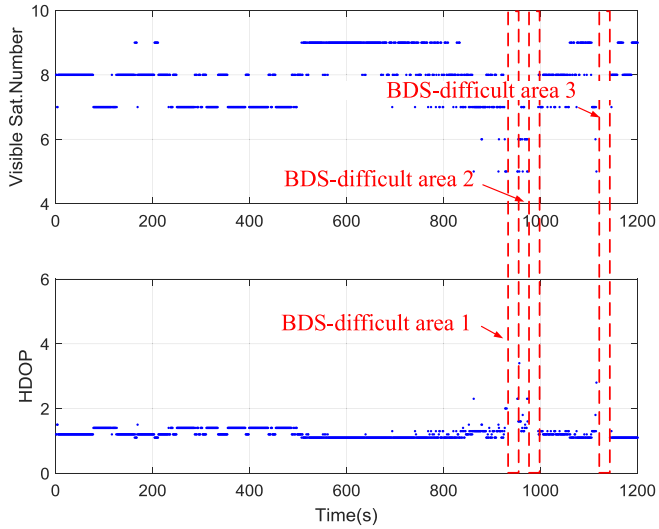

Fig. 16. The number of visible satellites and HDOP values.

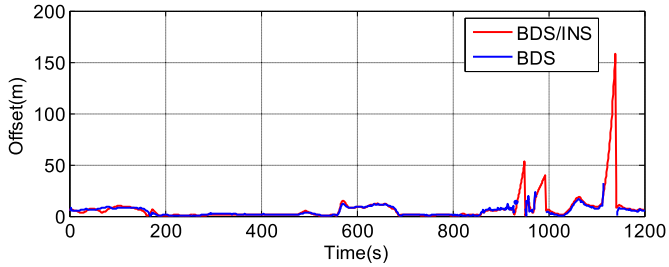

Fig. 17. Comparison of BDS/INS positioning offset and BDS positioning offset with the real track.

BDS-generated position is obtained from pseudorange measurements computed in the SPP mode.

Fig. 16 shows the number of visible satellites and the HDOP for the BDS solutions. One can see that the number of visible satellite drops during the latter part of the test, and the HDOP value correspondingly increases.

A HDOP value smaller than 1.5 is adopted as the threshold for deciding on the degree of BDS availability. When the number of visible satellite is less than 6 or the HDOP is greater than 1.5, the BDS signals are assumed to be "unavailable". The perpendicular distance threshold for the application of MM is assumed to be 25 m in this paper, commensurate with the BDS SPP accuracy.

3) Evaluation of BDS/INS Integrated Positioning Method: In order to overcome the problem that satellite signals cannot be always tracked in difficult areas, the GNSS/INS integrated positioning system is always used to obtain the navigation solution. The results from the BDS/INS integrated system are shown in Fig. 17. The blue solid line indicates the offset between the BDS positioning result and the real track, while the red line is the offset between the BDS/INS solution and the real track. It can be seen that the BDS/INS result is almost the same as that of BDS system in BDS-available areas, while the offset grows with time in the three BDS-difficult areas.

Fig. 18 compares the positioning performance of the BDS/INS system and the real track information for the three

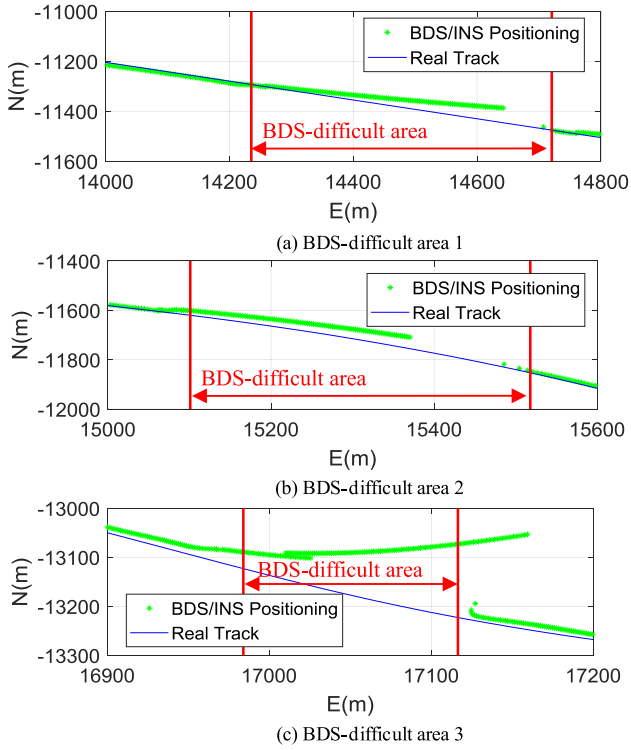

Fig. 18. Comparison of BDS-only and BDS/INS positioning results.

BDS-difficult areas. The blue solid line indicates the real track, while the green line with the symbol "∗" is the positioning result from the BDS/INS integrated system, where the output rate is 5 Hz. BDS signal difficult areas have been marked between the two red lines. When the train is in the BDS-difficult area, only INS can operate, and the gyroscope and accelerometer biases accumulate rapidly with time. This has a serious effect on the train positioning performance. The attitude error is hard to constrain during the long BDS outages and delivers incorrect results even after the BDS signals are reacquired, as shown in the latter part of Fig. 16.

4) Evaluation of Odometer/INS Integrated Positioning Method: As show in Fig. 17 and Fig. 18, INS performance cannot fill the BDS gap, and the odometer is used to improve the positioning accuracy for short BDS-difficult areas. The results of the odometer/INS integrated system are shown in Fig. 19. As the performance of the odometer/INS system is influenced by the estimated attitude, the evaluation is conducted for the straight line segment and the curve line segment. Both straight and curve parts are selected with a period of 2 minutes.

Plot (a) shows the odometer/INS positioning result in the straight line. The blue solid line indicates the real track, while the green line with the symbol "△" is the positioning result of the odometer/INS integrated system in 2 mins, where the output rate is 1 Hz in the top plot. The bottom plot shows the offset between the odometer/INS positioning results and the real track. It can be seen that the offset remains smooth within a two minute period and the offset is less than 2 m.

However, the results of the odometer/INS integrated system in the curve line segment cannot compete with those in the

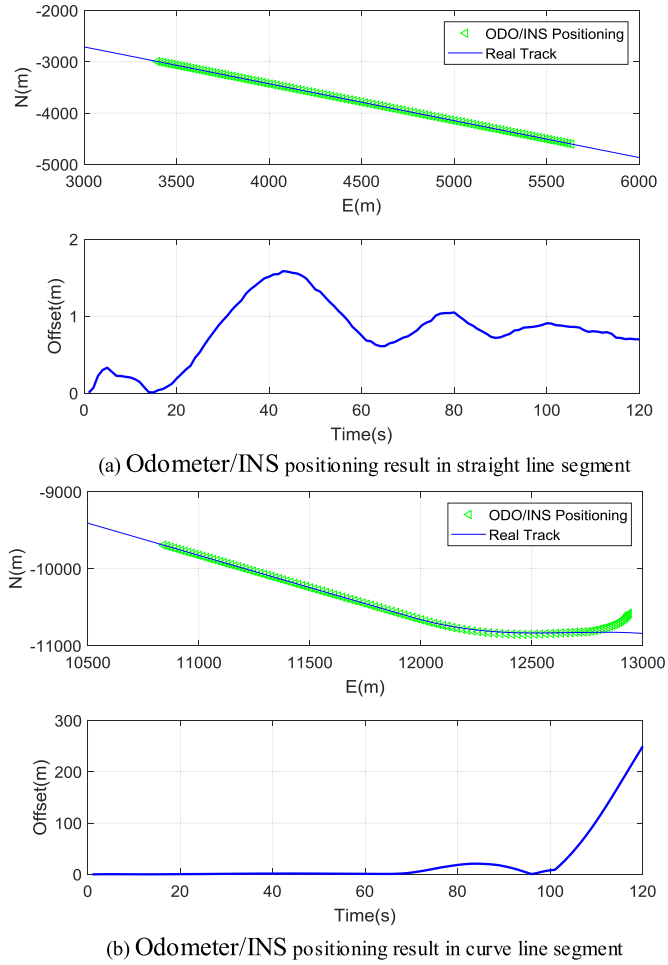

Fig. 19. Odometer/INS positioning result evaluation.

straight line segment. Plot (b) shows the trajectory and offset of the odometer/INS integrated system in the curve line segment. The curve line exists in the latter part of the 2 minute test, and one can see the offset between the estimated train position and the real track increase with the curve.

By comparing the results of the odometer/INS integrated system in the straight line and curve line segments, it can be seen the augmentation of the odometer can help smooth the positioning result during BDS gaps in short and straight line scenarios.

5) Evaluation of MM-Augmented BDS/INS/Odometer Integrated Method: It has been shown that the integrated odometer/INS system could help overcome BDS gaps in short and straight train operational scenarios, and MM can help reduce the error between estimate position and the real track. It is possible to use the BDS/INS/odometer/MM method instead of the BDS/INS and odometer/INS integrated systems to provide an accurate and continuous navigation solution. Fig. 20 compares the positioning performance of the proposed BDS/INS/odometer/MM system and the real track information. The blue solid line indicates the real track, while the green line with the symbol "△" is the positioning result from the BDS/INS/odometer/MM integrated system. When the BDS signals are available, the BDS, INS, odometer and MM are integrated to obtain the final position result, with a high update rate of 123 Hz. When the train is in a BDS-obstructed area, the INS, odometer and MM are still functional. In this case the odometer and INS are integrated with the assistance of MM to provide a continuous positioning capability, with an output rate of 123 Hz. From Fig. 20 one can see that the BDS/INS/odometer/MM integrated system can be seamlessly switched to the INS/odometer/MM mode in the case when BDS signals are blocked, and the matching points are in good agreement with the real railway track.

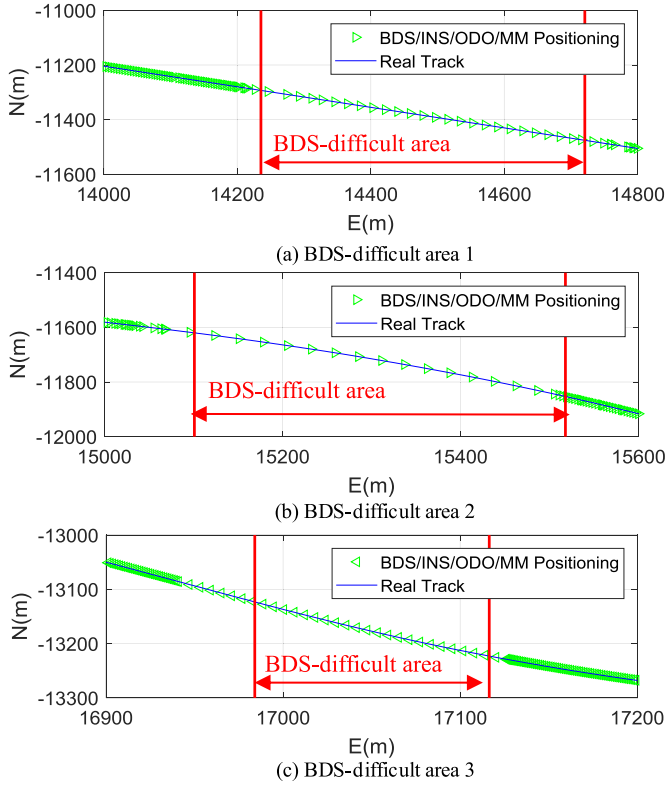

Fig. 20. Comparison of BDS/INS/odometer/MM positioning results and real track information.

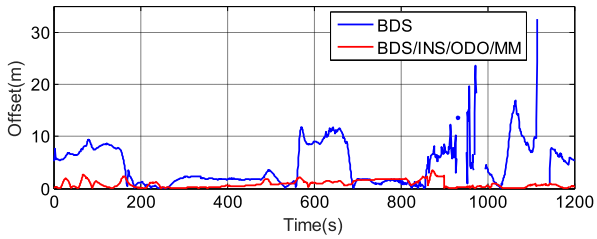

Fig. 21. Comparison of BDS/INS/odometer/MM positioning result and BDS positioning result corresponding to the real track.

Fig. 21 compares the offset of the BDS positioning result with that of the BDS/INS/odometer/MM system. The blue solid line indicates the offset between the BDS result and the real track information, while the red solid line shows that of the BDS/INS/odometer/MM system. Note that the positioning results of the BDS/INS/odometer/MM system have less offset with respect to the real track than the BDS/INS positioning re-

TABLE I
EVALUATION OF PROPOSED BDS/INS/ODOMETER/MM INTEGRATED SYSTEM AND CONVENTIONAL ODOMETER/BALISE INTEGRATED SYSTEM (UNIT: m)

	BDS/INS/odometer/MM	Odometer/balise
MEAN (m)	0.78	0.89
STD (m)	0.65	2.73
RMS (m)	1.02	3.32

sults and can further constrain the error of the INS, and hence improve the accuracy of the integrated navigation system in BDS-difficult areas.

The mean error, standard derivation error (STD) and root mean square error (RMS) of the proposed BDS/INS/odometer/MM system have been computed and compared with the conventional odometer/balise integrated system in Table I. It can be seen the RMS of the proposed system is 1.02 m, which satisfies the current train positioning accuracy requirement mentioned in Section II, and much higher than the current applied odometer/balise train determination system with RMS of 3.32 m.

VI. CONCLUSIONS

This paper proposed an integrated navigation system based on BDS, INS, odometer and MM sensors and techniques in order to provide a continuous and reliable train positioning service in LDL railway operations. The proposed navigation system has two operating scenarios: open-sky and BDS-obstructed environments. In the open-sky environment, the BDS signals are available to provide accurate train positioning, the BDS, odometer and INS are integrated to correct the INS sensor errors via a FKF. The navigation system switches to the odometer/INS integration mode when the train runs close to or enters a BDS-difficult area, such as tunnels, valleys, bridges or steep hillsides.

Furthermore, the MM algorithm can significantly reduce the excessive errors of BDS SPP solutions and help determine the train location on the rail track. To evaluate the proposed navigation system, a real experiment was conducted on the Qinghai-Tibet railway in the western region of China. The experimental results confirm that the proposed system can provide a seamless and continuous positioning service in both open-sky and BDS-obstructed environments. Compared with a conventional odometer/balise method, or BDS-only and BDS/INS navigation systems, the proposed system shows an obvious improvement performance, especially in BDS-difficult areas.

VII. FURTHER WORK

The proposed train multi-sensor navigation system is based on BDS, INS, odometer and MM technologies. The accuracy of the proposed navigation system is most influenced by BDS positioning accuracy. In this paper, the BDS positioning results is generated using the SPP mode, which can only achieve few meter-level accuracy for kinematic positioning applications. Therefore further work could be conducted to improve the BDS positioning accuracy using the carrier phase-based precise point positioning methods or double-differenced differential positioning in order to satisfy higher accuracy applications.

REFERENCES

[1] J. Pore, "A Hi-tech solution for low-density lines," *Transp. Res. Part C*, vol. 42, no. 12, pp. 36–46, 2002.

[2] A. Białoń and P. Gradowski, "Low market density lines for ERTMS regional system," *Arch. Transp. Syst. Telematics*, vol. 2, no. 2, pp. 37–40, 2009.

[3] B. Stadlmann, "Automation of operational train control on regional branch lines by a basic train control," in *Proc. IEEE Intell. Transp. Syst. Conf.*, Toronto, Canada, 2006, pp. 50–54.

[4] P. Ernest, R. Mazl, and L. Preucil, "Train locator using inertial sensors and odometer," in *Proc. IEEE Intell. Veh. Symp.*, Parma, Italy, 2004, pp. 860–865.

[5] L. Pugi, M. Rinchi, M. Malvezzi, and G. Cocci, "A multipurpose platform for HIL testing of safe relevant railway subsystem," in *Proc. Conf. IEEE/ASME Adv. Intell. Mechatron.*, Monterey, CA, USA, 2005, pp. 282–288.

[6] *Next Generation of Train Control Systems—WP2-ETCS CBTC Investigation of Operational and Functional Consistencies and Differences, Seventh Framework Programme*, NGTC, Brussels, Belgium, 2016.

[7] *CTCS-3 Train* Control System Operation Standard-Balise Opera*tion and* Installation Manual, China Railway, Beijing, China, 2012.

[8] P. Gurnik, "Next generation train control (NGTC): More effective railways through the convergence of main-line and urban train control systems," *Transp. Res. Procedia*, vol. 14, pp. 1855–1864, 2016.

[9] B. Allotta, L. Pugi, A. Ridolfi, M. Malvezzi, G. Vettori, and A. Rindi, "Evaluation of odometry algorithm performances using a railway vehicle dynamic model," *Veh. Syst. Dyn.*, vol. 50, no. 5, pp. 699–724, 2012.

[10] A. Neri, S. Sabina, and U. Mascia, "GNSS and odometry fusion for high integrity and high availability train control systems," in *Proc. 28th Int. Tech. Meet. Satellite Div. Inst. Navig.*, Tampa, FL, USA, 2015, pp. 639–648.

[11] S. Han and J. Wang, "Quantization and colored noises error modeling for inertial sensors for GPS/INS integration," *IEEE Sensors J.*, vol. 11, no. 6, pp. 1493–1503, Jun. 2011.

[12] M. A. Jaradat and M. F. Abdel-Hafez, "Enhanced, delay dependent, intelligent fusion for INS/GPS navigation system," *IEEE Sensors J.*, vol. 14, no. 5, pp. 1545–1554, May 2014.

[13] T. Zhang and X. Xu, "A new method of seamless land navigation for GPS/INS integrated system," *Measurement*, vol. 45, no. 4, pp. 691–701, 2012.

[14] A. Acharya, S. Smita, and T. Ghoshal, "Train localization and parting detection using data fusion," *Transp. Res. C*, vol. 19, no. 1, pp. 75–84, 2011.

[15] H. Gao, B. Chen, J. Wang, K. Li, J. Zhao, and D. Li, "Object classification using CNN-based fusion of vision and LIDAR in autonomous vehicle environment," *IEEE Trans. Ind. Informat.*, vol. 14, no. 9, pp. 4224–4231, Sep. 2018, doi: 10.1109/TII.2018.2822828.

[16] G. Xie, H. Gao, L. Qian, B. Huang, K. Li, and J. Wang, "Vehicle trajectory prediction by integrating physics- and maneuver-based approaches using interactive multiple models," *IEEE Trans. Ind. Informat.*, vol. 65, no. 7, pp. 5999–6008, Jul. 2018.

[17] H. Gao, X. Zhang, L. An, Y. Liu, and D. Li, "Relay navigation strategy study on intelligent drive on urban roads," *J. China Univ. Posts Telecommun.*, vol. 23, no. 2, pp. 79–90, 2016.

[18] M. Quddus and S. Washington, "Shortest path and vehicle trajectory aided map-matching for low frequency GPS data," *Transp. Res. C*, vol. 55, pp. 328–339, 2015.

[19] S. Saab, "A map matching approach for train positioning part I: Development and analysis," *IEEE Trans. Veh. Technol.*, vol. 49, no. 2, pp. 467–475, Mar. 2000.

[20] K. Gerlach and C. Rahmig, "Multi-hypothesis based map-matching algorithm for precise train positioning," in *Proc.12th Int. Conf. Inf. Fusion*, Seattle, WA, USA, 2009, pp. 1363–1369.

[21] O. Heirich, "Bayesian train localization with particle filter, loosely coupled GNSS, IMU, and a track map," *J. Sens.*, vol. 2016, pp. 1–15, 2016.

[22] S. Soderholm, M. Bhuiyan, S. Thombre, L. Ruotsalainen, and H. Kuusniemi, "A multi-GNSS software-defined receiver: Design, implementation, and performance benefits," *Ann. Telecommun.*, vol. 71, nos. 7/8, pp. 1–12, 2016.

[23] M. Jonas, "Integrity of GNSS position solution for safety related applications," in *Proc. 28th Int. Tech. Meet. Satellite Div. Inst. Navig.*, Tampa, FL, USA, 2015, pp. 1603–1607.
[24] D. Salmon and D. Bevly, "An exploration of low-cost sensor and vehicle model solutions for ground vehicle navigation," in *Proc. IEEE/ION Position, Location Navig. Symp.*, Monterey, CA, USA, 2014, pp. 462–471.
[25] China Satellite Navigation Office. (2013). *BeiDou Navigation Satellite System Open Service Performance Standard (Version 1.0)*. [Online]. Available: http://www.beidou.gov.cn/attach/2013/12/26/20131226298ff2928cc34e45b4714a6ac0e14a1c.pdf
[26] E. Hemerly and V. Schad, "Implementation of a GPS/INS/odometer navigation system," in *Proc. ABCM Symp. Ser. Mechatron.*, 2008, vol. 3, pp. 519–524.
[27] Y. Zheng and P. Cross, "Integrated GNSS with different accuracy of track database for safety-critical railway control systems," *GPS Solutions*, vol. 16, no. 2, pp. 169–179, 2012.
[28] S. Gao, Y. Zhong, X. Zhang, and B. Shirinzadeh, "Multi-sensor optimal data fusion for INS/GPS/SAR integrated navigation system," *Aerosp. Sci. Technol.*, vol. 13, no. 45, pp. 232–237, 2009.
[29] C. Lo, J. P. Lynch, and M. Liu, "Distributed reference-free fault detection method for autonomous wireless sensor networks," *IEEE Sensors J.*, vol. 13, no. 5, pp. 2009–2019, May 2013.
[30] X. Li and W. Zhang, "An adaptive fault-tolerant multisensory navigation strategy for automated vehicles," *IEEE Trans. Veh. Technol.*, vol. 59, no. 6, pp. 2815–2829, Jul. 2010.
[31] N. A. Carlson and M. P. Berarducci, "Federated Kalman filter simulation results," *NAVIG., J. U.S. Inst. Navig.*, vol. 41, no. 3, pp. 297–321, 1994.
[32] N. A. Carlson, "Federated filter for computer-efficient, near-optimal GPS integration," in *Proc. IEEE Position Location Navig. Symp.*, Atlanta, GA, USA, 1996, pp. 306–314.

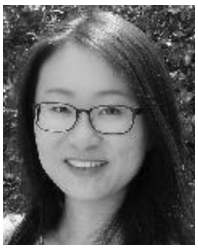

Wei Jiang received the Ph.D. degree from the School of Civil and Environmental Engineering, University of New South Wales, Sydney, N.S.W., Australia. She is currently an Associate Professor with the School of Electronic and Information Engineering, Beijing Jiaotong University, Beijing, China. Her current research interests include multisensor integration, and, in particular, the implementation of new navigation and data-fusion algorithms.

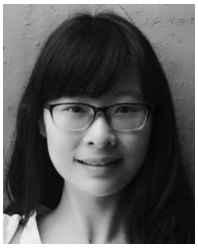

Sirui Chen received the B.S. and M.S. degrees from Beijing Jiaotong University, Beijing, China, in 2015 and 2018, respectively. She is currently with the College of Intelligent Transportation, Zhejiang Institute of Communications, Zhejiang, China. Her current research interests include optimal train localization and intelligent transportation system.

Baigen Cai (SM'13) received the B.S., M.S., and Ph.D. degrees in traffic information engineering and control from Beijing Jiaotong University, Beijing, China, in 1987, 1990, and 2010, respectively. From 1998 to 1999, he was a Visiting Scholar with Ohio State University. Since 1990, he has been with the Faculty of the School of Electronic and Information Engineering, Beijing Jiaotong University, where he is currently a Professor and Chief with the Science and Technology Division. His research interests include train control system, intelligent transportation system, GNSS navigation, multisensor fusion, and intelligent traffic control.

Jian Wang (M'10) received the B.S., M.S., and Ph.D. degrees from Beijing Jiaotong University, Beijing, China, in 2000, 2003, and 2007, respectively. From 2007 to 2010, he was a Lecturer with the School of Electronic and Information Engineering, Beijing Jiaotong University, where he is currently an Associate Professor. His professional interests include train control system, new GNSS applications in railway, and other ITS technologies.

Wei ShangGuan (M'14) received the B.S., M.S., and Ph.D. degrees from Harbin Engineering University, Harbin, China, in 2002, 2005, and 2008, respectively. From 2008 to 2011, he was a Lecturer with the School of Electronic and Information Engineering, Beijing Jiaotong University, Beijing, China. From 2013 to 2014, he was an Academic Visitor with University College London. He is currently an Associate Professor and Supervisor of Master with Beijing Jiaotong University. His professional research interests include train control system (CTCS/ETCS/ERTMS), system modeling, simulation, and testing, GNSS (GPS, Galileo, GLONASS, and BDS)/GIS, integrated navigation, intelligent transportation system, and cooperative vehicle infrastructure system of China.

Chris Rizos is currently an Emeritus Professor with the School of Civil and Environmental Engineering, University of New South Wales, Sydney, N.S.W., Australia. He is an author/coauthor of more than 650 journal and conference papers. Since 1985, his research interests include the technology and applications of GPS. He was a Past President of the International Association of Geodesy, a member of the Executive and Governing Board of the International GNSS Service, and the President of the Australian Institute of Navigation.